

1 **Test**

2 **Alexander Beck¹, Jan Henneberger¹, and Ulrike Lohmann¹**

3 ¹Institute for Atmospheric and Climate Sciences, ETH Zurich, Zurich, Switzerland

4 **Key Points:**

- 5 • In-situ measurements of microphysical cloud properties with a holographic Imager
6 • Influence of in-situ cloud observations at mountain top stations by ground based ice
7 enhancement processes
8 •

9 **Abstract**

10 In-situ cloud observations at mountain-top research station regularly measure ice crystal
 11 number concentrations (ICNCs) orders of magnitudes higher than expected from mea-
 12 surements or simulations of ice nuclei particle concentrations. Several studies suggest
 13 mountain-top in-situ measurements are influenced by surface-based ice-enhancement pro-
 14 cess, e.g. blowing snow, hoar frost or riming on snow covered trees, rocks and the remain-
 15 ing snow surface. A strong influence of in-situ observations on mountain-top stations by
 16 surface-based ice-enhancement processes may limit relevance of such measurements and
 17 could have an impact on orographic clouds.

18 This study assesses the influence of surface-based ice-enhancement processes on
 19 in-situ cloud observations at the Sonnblick Observatory in the Hohen Tauern Region,
 20 Austria. Vertical profiles of ICNCc above a snow covered surface were observed up to a
 21 height of 10 m. In clouds, the ICNCs decreased by at least a factor of two in the observed
 22 height interval. During a cloud-free period the ICNC decreases from several hundreds per
 23 liter near the ground to 10 per liter at a height of 10 m.

24 Information on wind, spectra and habit...

25 For one case study a correlation between ICNC and horizontal wind speed was ob-
 26 served for wind speeds below 10 m s^{-1} . for wind , a dependency of the ICNC on the hor-
 27 izontal and vertical wind speed was observed. These observations strongly suggest that
 28 mountain-top in-situ measurements are strongly influenced by surface-based ice-enhancement
 29 processes.

30 **1 Introduction**

31 The microphysical properties (e.g. phase composition, cloud particle number con-
 32 centrations) and cloud processes are key parameters for the clouds lifetime, the cloud ex-
 33 tent, as well as the intensity of precipitation they produce [Rotunno and Houze, 2007]. For
 34 example, the phase composition influence the radiative properties of midlevel clouds in
 35 the temperature range between 0 to -35 °C. A pure ice cloud in this temperature regime
 36 reflects 17 W m^{-2} more radiation than an pure liquid cloud [Lohmann, 2002]. A well rep-
 37 resentation of orographic mixed-phase clouds is therefore crucial for accurate weather pre-
 38 dictions in alpine terrain and improved climate models.

39 In-situ measurements are important to improve our understanding of microphysical
 40 properties and fundamental processes of orographic mixed-phase clouds [Baumgardner
 41 et al., 2011] and are frequently conducted at mountain-top research stations. Despite an
 42 improved understanding on the origin of ice crystals from nucleation (citation!!!!) as well
 43 as from secondary ice-multiplication processes [Field et al., 2017], the source of most of
 44 the ice crystals observed at mountain-top stations and their impact on the development of
 45 the cloud remains an enigma (citation!!!!).

46 In-situ observations with aircraft usually observe and ICNC on the order of $1\text{-}101^{-1}$
 47 [Gultepe et al., 2001], whereas at mountain-top research stations (e.g. Elk Mountain, USA
 48 or Jungfraujoch, Switzerland) or near the snow surface in the Arctic ICNCs of several
 49 hundreds to thousands per liter are frequently reported [Rogers and Vali, 1987; Lachlan-
 50 Cope et al., 2001; Lloyd et al., 2015]. Secondary ice multiplication processes like frag-
 51 mentation [Rangno and Hobbs, 2001] or the Hallett-Mossop process [Hallet and Mossop,
 52 1974] are usually ruled out as the source for the observed ice crystals due to the lack of
 53 large ice crystals, respectively large cloud droplets or the wrong temperature range. In-
 54 stead surface-based ice-enhancement processes are proposed to produce such enormous
 55 ICNCs. Rogers and Vali [1987] suggested two possible processes as a source for the ob-
 56 served ICNC: riming on trees, rocks and the snow surface or the lifting of snow particles
 57 from the surface, i.e. blowing snow. In addition, Lloyd et al. [2015] suggested hoar frost

as a wind independent, surface-based ice-enhancement process to cause ICNCs larger than 100l^{-1} for which they didn't observe a wind dependency as expected for blowing snow. Although different studies are strife about the mechanisms to explain the measured high ICNCs, they agree on an strong influence by surface-based processes.

While the influence of mountain-top measurements by surface-based processes is widely accepted, the impact of re-suspended ice crystals on the development of super-cooled orographic clouds, e.g. a more rapid glaciation and enhanced precipitation, has not been studied extensively [Geerts *et al.*, 2015]. If the proposed surface-based ice-enhancement processes have the potential to impact the development of a cloud depends primarily on the penetration depth of the reseuspended particle into a cloud, i.e. the maximum height above the surface to which the particles get lifted.

The height dependency of blowing snow has been studied in the context of snow redistribution ("snow drift") and reduced visibility due to the re-suspended ice crystals by observing ice crystals up to several meters above the snow surface [Schmidt, 1982; Nishimura and Nemoto, 2005]. It has been reported that blowing snow occurs above a wind speed threshold that varies between 4 m s^{-1} and 13 m s^{-1} [Bromwich, 1988; Li and Pomeroy, 1997; Mahesh et al., 2003; Déry and Yau, 1999]. Besides the wind speed, the concentration of blowing snow depends on the snowpack properties () and on the atmospheric conditions (current temperature, humidity) [Vionnet et al., 2013]. Nishimura and Nemoto [2005] observed the ICNC up to a height of 9.6 m and found that the ICNCs usually decrease to as low as 1-10 particles per liter. During a precipitation event, the relative importance of the small ice crystals below $< 100 \mu\text{m}$ decreases from nearly 100 % at 1.1 m to below 20 % at 9.6 m. The rapid decrease of ICNCs with height observed by these studies may limit the impact of blowing snow on orographic clouds. However, most of these studies were conducted in dry air conditions where ice crystals undergo rapid sublimation [Yang and Yau, 2008], which may limit the applicability of these results.

Lloyd *et al.* [2015] suggested that vapor grown ice crystals on the crystalline surface of the snow cover, i.e. hoar frost, may be detached by mechanical fracturing due to turbulence independent of wind speed. To our knowledge only one modelling study exists, which asses the impact of haor frost on the development of a cloud. Farrington *et al.* [2015] implemented a flux of surface hoar crystals in the WRF (Weather Research and Forecasting) model based on a frost flower aerosol flux to simulate ICNCs measured at the Jungfraujoch by Lloyd *et al.* [2015]. They concluded, that the surface-based ice-crystals have a limiting impact on orographic clouds because the ice crystals are not advected high into the atmosphere. However, more measurements of ice-crystal fluxes from the snow covered surface are necessary to simulate the impact of surface-based ice-crystal enhancement processes on the development of orographic clouds [Farrington *et al.*, 2015].

In contrast to these finding, several remote sensing (i.e. satellite, lidar and radar) studies measured ice crystals advected as high as 1 km above the surface, which suggest an impact of surface-originated ice-crystals on clouds. Satellite observations of blowing snow from MODIS and CALIOP over the Antarctica [Palm *et al.*, 2011] observed layer thickness up to 1 km with an average thickness of 120 m for all observed blowing snow events. Similar observations from lidar measurements exist from the South Pole with an observed layer thickness of ice crystals of usually less than 400 m, but some rare cases when a subvisual layer exceeded a height of 1 km [Mahesh *et al.*, 2003]. However, a possible suspension of clear-sky precipitation could not be ruled out as a source of the observed ice crystal layers. Observations of layers of ice crystals from radar measurements on an aircraft in the vicinity of the Medicine Bow Mountains [Vali *et al.*, 2012] observed ground-layer snow clouds which where most of the time not visually detectable but produced a radar signal. Resuspended ice crystals from the surface or riming of cloud droplets at the surface can be the origin of the ice crystals in such ground-layer snow clouds. Geerts *et al.* [2015] presented evidence for ice crystals becoming lofted up to 250 m in the atmosphere by boundary layer separation behind terrain crests and by hy-

draulic jumps. Also evidence that ice crystals from the surface may lead to the glaciation of supercooled orographic clouds and enhanced precipitation were found. However, *Geerts et al.* [2015] also mention the limitation of radar and lidar measurement to separate the small ice crystals produced by surface processes from the larger falling snow particles and more abundant cloud droplets. They even concluded, that "to explore BIP (blowing snow ice particle) lofting into orographic clouds, ice particle imaging devices need to be installed on a tall tower, or on a very steep mountain like the Jungfraujoch".

In this study we assess the influence of surface-based ice-enhancement processes on in-situ cloud observations at mountain-top stations and the a potential impact on orographic mixed-phase clouds. Therefore, vertical profiles of the ICNC up to a height of 10 m above the surface are observed for the first time in cloud at the Sonnblick Observatory. Ice crystals are recorded with the holographic imager HOLIMO, capable of observing ice crystals larger than 25 μm [Beck *et al.*, 2017].

2 Field Measurements at the Sonnblick Observatory

2.1 Site description

This field campaign was conducted at the Sonnblick Observatory (SBO) situated at the summit of Mt. Sonnblick at 3106 masl (12°57'E, 47°3'N) in the Hohen Tauern National Park in the Austrian Alps. The SBO is a meteorological observatory operated all year by the ZAMG (Central Institute for Meteorology and Geodynamics). On the East and South the SBO is surrounded by large glacier fields with a moderate slope, whereas on the Northeast a steep wall of approximately 800 m descends to the valley (Fig. 1, right). Part of the SBO is a 15 m high tower used for meteorological measurements by the ZAMG. The data presented in this paper was collected during a field campaign in February 2017.

2.2 Instrumentation

The microphysical properties of clouds, hydrometeors and resuspended particles from the surface were observed with the holographic Imager HOLIMO, which is part of the HoloGondel platform [Beck *et al.*, 2017]. The holographic Imager was mounted on an elevator that was attached to the meteorological tower of the SBO (Fig. 2) to obtain vertical profiles of the microphysical properties up to a height of 10 m above the surface where the platform was repeatedly positioned at five different heights as indicated in Figure 2. The holographic imager HOLIMO had a distance of approximately 1.5 m from the tower on the east-northeast side of the tower (Fig. 1, right). The holographic imager HOLIMO captures the information of cloud particles in a three-dimensional volume on a single image. In this study a sample volume of 16 cm^3 with a length of 6 cm along the optical axis was examined. The data is averaged over 50 holograms and a total volume of 800 cm. The open source software HoloSuite [Fugal, 2017] is used to reconstruct the in-focus images of the particles. Particles smaller than 25 μmm are classified as liquid droplets, whereas particles larger than 25 μmm are separated in liquid droplets and ice crystals based on the shape of their 2D image. Similar to a study by *Schlenzeck and Fugal* [2017] the ice crystals were further visually classified into three different groups: regular, irregular and aggregates. Because the visual classification of several thousands of ice crystals is time consuming this sub-classification of ice crystals was done only for the profiles on February 17th.

Meteorological data are available from the measurements by the ZAMG and the HoloGondel platform. The ZAMG measures one minute averages of temperature, relative humidity and horizontal wind speed and direction at the top of the meteorological tower. Snow cover depth is daily manually observed by the operators of the SBO. Based on these measurements the change of the snow cover is calculated. However, this calculation includes all the changes in the snow cover depth, e.g. snow drift, sublimation, melting

160 and fresh snow. Daily measurements of the total precipitation are available on the North
 161 and South side of the SBO. A ceilometer located in the valley on the North of the SBO
 162 measured the cloud base and cloud depth. An additional 3D Sonic Anemometer, which is
 163 part of the HoloGondel platform [Beck *et al.*, 2017], was mounted at the top of the meteo-
 164 rological tower. However, data is only available occasionally, because most of the time the
 165 heating of the Anemometer was not sufficient enough to prevent the build up of rime on
 166 the measurement arms.

167 3 Results

168 The data presented were observed on 4 February and 17 February 2017. Figure 3
 169 and 4 show an overview on the meteorological conditions on both days. The main differ-
 170 ence is the wind direction, which was South-West on 4 February and North on 17 Febru-
 171 ary.

172 3.1 4 February 2017

173 On 4 February a low pressure system moved eastwards from the Atlantic Ocean over
 174 northern France to western Germany, where it slowly dissipated. Influenced by this low
 175 pressure system the wind at the SBO predominantly came from West-Southwest and wind
 176 speeds between 10 and 25 m s⁻¹. In the late afternoon around 1900 UTC, when the low
 177 pressure system dissipated over western Germany, the wind direction changed to North
 178 and wind speeds decreased to a minimum of 5 m s⁻¹. After 1900 UTC wind speed in-
 179 creased again to up to 15 m s⁻¹. Starting from 0800 UTC the SBO was in cloud except
 180 for a short time interval between 1910 and 2020 UTC. The temperature didn't change
 181 much during the day and stayed between -10 and -9 °C until 1900 UTC when the wind
 182 direction changed to North and the temperature decreased to -11 °C at 22 UTC.

183 Between 0830 and 2200 UTC, a total of 24 vertical profiles were obtained. Because
 184 no data is available from the 3D Sonic Anenometer, only one minute averages of tem-
 185 perature, wind speed and direction are available from the ZAMG measurements (Fig. 3).
 186 Most of the profiles were obtained when the station was in cloud expect for four profiles
 187 between 1910 and 2020 UTC as indicated in Figure 3. The ICNC as a function of height
 188 summarized over 24 vertical profiles obtained on 4 February is shown in Figure 5. The
 189 ICNC reaches a maximum at 2.5 m above the surface. Compared to this maximum, the
 190 mean ICNC at a height of 10 m decreases by a factor of two and the median ICNC even by
 191 a factor of four. These observations suggest an influence of the measurements close to the
 192 snow surface by surface based ice crystal enhancement processes and a rapid decrease of
 193 the ICNC with height.

194 Figure 6 shows four time periods representing different conditions during the 4 Febru-
 195 ary. For the vertical profiles obtained between 1910 and 2010 UTC (Fig. 6 first row),
 196 when the SOB was not in cloud, the ICNCs have their maximum at a height of 2.5 m.
 197 The maximum ICNC at this height reaches up to 600 l⁻¹. For three of the profiles, the
 198 ICNC decrease by more than a factor of 5 from over 100 l⁻¹ at 2.5 m to less than 20 l⁻¹ at
 199 10 m. The mean ICNC decreases from around 100 l⁻¹ at 2.5 m to 10 l⁻¹ at 10 m (Fig. 6,
 200 right panel in the first row). The large extend of the shaded area at 2.5 m represents the
 201 high variability of the ICNC even when the data is averaged over 50 holograms. Because
 202 the SBO was not in cloud during this time period, these measurements strongly suggest an
 203 influence by surface based processes at a wind speed of less than 10 m s⁻¹ of up to several
 204 hundreds of ice crystals per liter at a height of 2.5 m.

205 Between 2030 and 2200 UTC (Fig. 6 second row), when the SBO was in cloud
 206 again, the vertical profiles of the ICNC show a similar tendency as in the cloud free pe-
 207 riod. The maximum of the ICNC was observed at a height of 4.1 m and the ICNC de-
 208 creases consistently for all four profiles with height above the observed maximum. The

209 boxplot on the right of Figure 6 shows that the mean of the ICNC decreases by a factor
 210 of 9 from its maximum at 4.1 m to its minimum at 10 m. This decrease is in the same or-
 211 der of magnitude as in the cloud free case discussed above. Assuming that the observed
 212 ICNC at 10 m is representative for the cloud without surface influence, the surface-based
 213 processes contribute with several hundreds of ice crystals per liter to the measurements at
 214 2.5, 4.1 and 6.0 m. This surface-based contribution is in the same order of magnitude as
 215 the total measured ICNCs in the cloud free period observed between 1910 and 2020 UTC.
 216 The influence extends to a height of 6.0 m, which is probably due to an increased wind
 217 speed of up to 15 m s^{-1} .

218 The highest ICNCs were observed in the time period between 1200 and 1500 UTC
 219 (Fig. 6 second row) when also the wind speed reaches its maximum of 25 m s^{-1} . The box-
 220 plot for this time interval shows a maximum ICNC at 2.5 m in the range of 500 to 900 l^{-1}
 221 and a decrease by a factor of 2 within 7.5 m. This decrease is much lower than observed
 222 in the previous time interval and is most likely due to the high wind speeds. Between dif-
 223 feren profiles the ICNC changed by a factor of, however, the trend of a decreasing ICNC
 224 with height was observed consistently for all profiles.

225 In the morning between 0830 and 1100 UTC the observed ICNCs (Fig. 6 first row)
 226 are much lower than between 1200 and 1500 UTC, although wind speed was as high as
 227 20 m s^{-1} . A possible reason is the history of the snowpack before 04 February 2017. The
 228 last snow fall was observed on ?? February 2017 and most of the loose ice crystals on top
 229 of the snowpack possibly already have been blown away. Therefore, higher wind speeds are
 230 necessary to resuspend ice crystals from the snowpack.

231 To get an estimate of the correlation between wind speed and ICNC, the ICNC
 232 is averaged over a time interval of 1 min and compared to the maximum wind speed in
 233 the corresponding 1 min time interval observed by the SBO on top of the meteorological
 234 tower. Maximum wind speed is used rather the average wind speed, because it is expected
 235 that the gusts, i.e. the highest wind speed in an time interval are most relevant for resus-
 236 pending ice crystals from the surface. For the time interval between 0830 an 1500 UTC
 237 when the wind direction was west-southwest (Fig 7, top) the ICNC shows no strong cor-
 238 relation is observed for wind speeds higher than 14 m s^{-1} . For the time interval bwetween
 239 1910 and 2230 UTC (Fig 7, bottom), when the wind direction was north, a much more
 240 pronounced dependency of the ICNC on wind speed is observed for wind speeds lower
 241 than 14 m s^{-1} . This is a possible indication that the ice crystal concentration reaches a sat-
 242 uration for wind speed larger than 14 m s^{-1} for the conditions on 04 February 2014.

243 3.2 17 February 2017

244 On 17 February a cold front over northern Europe was moving southwards causing
 245 mainly northerly flow across the alps and at the SBO. Wind speeds observed at the SBO
 246 in the time interval between 1800 and 2000 UTC were between 5 and 10 m s^{-1} (Fig. 4).
 247 In the same time interval temperature decreased by 1 K from -12.5 to -13.5°C . The SBO
 248 was in cloud starting from 1300 UTC with varying visibility between several meters up to
 249 several hundreds of meters. Some snow fall was observed in the afternoon between 1300
 250 and 1500 UTC.

251 For this day wind data of the 3D Sonic Anemometer are available, which allow a
 252 more detailed analysis of the correlation between the observed ICNC and wind speed. Un-
 253 fortunately, only four vertical profiles were obtained with the HoloGondel platform due to
 254 hardware problems with the computer of the platform. The first profile was measured in
 255 the morning at 1200 UTC when the SBO was not in cloud and no ice crystals were ob-
 256 served. Three more profiles were observed in the late afternoon starting from 1800 UTC.
 257 For these profiles the ice crystals have been classified by hand and subclassified in the
 258 three categories: regular, irregular and aggregates.

Figure 8 gives an overview on the three profiles observed in the late afternoon of 17 February. An ICNC of several hundreds was observed in the lowest height intervals with a maximum between 4.1 and 6.0 m. The minimal ICNC was consistently observed for all profiles at 10 m and was always below 150 l^{-1} . The decrease of the ICNC varies between a factor of 2 and 4. In general the observed profiles on this day are similar to the ones observed on 4 February between 2030 and 2200 UTC. This may be explained by very similar meteorological conditions. Wind direction was mainly from North to Northeast and wind speed varied between 5 and 10 m s^{-1} in both measurement intervals. Only temperature was slightly lower on 17 February.

In Figure 9 ICNCs are compared to various wind speeds. In contrast to the data of 4 February no correlation between ICNCs and the horizontal wind speed is observed. This holds true for the one minute average and maximum wind speed of the corresponding time interval observed by the SBO as well as the secondly average observed with the 3D Sonic Anemometer from the HoloGondel Platform. However, Figure 9c shows an increase of ICNC with the vertical wind speed.

All the ice crystals observed on 17 February were classified by hand a subclassification into irregular and regular ice crystals as well as aggregates was realized. The profiles of the subcategorized ICNCs and the relative abundance of these categories on the different heights are shown in Figure 10. ICNCs are dominated by irregular ice crystals, which is in good agreement with various other observations (citations). However, it is surprising to us that the relative importance of the irregular ice crystals stays constant with height or even increases. From surface based ice crystal enhancement processes irregular ice crystals are expected to enhance ICNCs near the surface. With increasing height this influence is expected to decrease and regular ice crystals to become more important. However, from this data a proportional decrease of the absolute number of regular and irregular ice crystals is observed. In Figure 11 the concentration of the different habits is correlated to the vertical wind speed observed. It shows that the ICNC of irregular ice crystals dependence more on wind speed.

Figure 12 shows the size distribution of regular and irregular ice crystals at three different heights. Whereas the shape of the size distribution of the irregular ice crystals doesn't vary much and only decreases with height, the size distribution of the regular ice crystals shows a stronger decrease of the larger ice crystals.

4 Discussion

4.1 Wind dependency of the observed ICNCs

The observations on 4 February and 17 February show a different correlation of the ICNC with wind speed. Whereas the ICNCs observed on 4 February show a dependency on horizontal wind speed below 14 m s^{-1} , this dependency is not observed for ICNCs on 17 February 9. However for the data on 17 February a correlation is observed with vertical wind speed available from the 3D Sonic Anemometer. Because the vertical wind speed is not available for 17 February possible reasons for this observation are speculative. Possibly the orography plays an important role for the wind speed dependency. The north side of the SBO is a steep wall of 800 m. Therefore, vertical winds may transport ice crystals from this wall up to the ridge of the mountain, where they finally become lifted into the air. A possible reason for the missing wind dependency on 4 February for horizontal wind speeds larger than 14 m s^{-1} is a saturation of the concentration of blowing snow.

In previous literature a wind dependency was observed for ICNCs smaller than $100 \mu\text{m}$, whereas larger ICNCs were wind independent [Lloyd *et al.*, 2015]. Blowing snow, respectively hoar frost were proposed as the underlying mechanisms for these observations. Based on our observations we propose that at mountain-top research station not only the

309 horizontal wind speed may play an important role for the resuspension of ice crystals from
 310 the surface, but also the vertical wind speed. This may be true particular for research sta-
 311 tions like the Jungfraujoch, Switzerland and SBO, Austria with their steep orography.

312 It has to be mentioned that various difficulties exist when it comes to observe the
 313 correlation between wind speed and ICNC. Firstly, ICNCs are usually compared to a si-
 314 multaneously measured wind speed. However, the observed ice crystals may have been
 315 resuspended some time before the measurement and transported in the air for a short time.
 316 In this case the simultaneously observed wind speed is not necessarily the driving force of
 317 the process of particle lifting. Secondly, wind and ICNC measurements may be performed
 318 at two different locations. Especially at mountain-top research station with its many struc-
 319 tures, local turbulence responsible for the resuspension of the observed ice crystals may be
 320 not well represented by such a wind measurement. Thirdly, the ICNC does not only de-
 321 pend on wind speed, but also on age of the snow cover and atmospheric conditions and a
 322 possible correlation may suppressed in a data set with different snowpack and atmospheric
 323 conditions.

324 4.2 Size distribution

325 To better understand if the observed ice crystals are mainly resuspended particles
 326 from the surface the ice crystals observed on 17 February were subclassified into three
 327 different habits: regular, irregular and aggregates and the results are compared to previous
 328 studies about blowing snow. Because the main focus of blowing snow studies was the re-
 329 distribution of snow and its effect on road visibility, avalanche danger as well as mass and
 330 energy balance, they usually focused on limited height intervals (<2 m) above the snow
 331 surface. To our knowledge only *Nishimura and Nemoto* [2005] conducted measurements
 332 of the properties of blowing snow up to a height of 9.6 m at Mizuho Station, Antarctica.
 333 However, it is important to keep in mind that also this study was conducted over a flat sur-
 334 face in dry air conditions.

335 It is known that the particle size distribution at different heights can be well rep-
 336 resented with two-parameter gamma probability density functions [*Budd*, 2013; *Schmidt*,
 337 1982]

$$338 f(d) = \frac{d^{\alpha-1}}{\beta^\alpha \Gamma(\alpha)} \exp\left(-\frac{\beta}{d}\right) \quad (1)$$

339 with the particle diameter d , the shape parameter α and the scale parameter β . The
 340 fitted results for 17 February are shown in Figure 13 for both regular and irregular ice
 341 crystals. The fits show close agreement with the data for both habits and all heights. The
 342 resulting shape parameter α and the mean diameter, represented by the product of the
 343 shape and scale parameter of the gamma-pdf, are plotted in Figure 14. The mean diameter
 344 of the regular ice crystals decreases with increasing height from 120 to 70 μm , whereas
 345 the mean diameter of the irregular ice crystals is constant at 100 μm . The shape factor
 346 for the irregular ice crystals also varies only little, whereas the shape factor for the regu-
 347 lar ice crystals increases from 5 to 7 at a height of 10 m. Compared to the results of ??
 348 the parameters of the size distribution of the regular ice crystals compare much better to
 349 the properties of blowing snow than the of irregular crystals. This is puzzling, because
 350 blowing snow has been observed to have dominantly ice crystals of irregular habits (cita-
 351 tion). For the data observed between 1910 and 2000 UTC on 4 February, which is clearly
 352 a blowing snow event, inspection of the ice crystal habit by eye confirm these results.

353 II is not believed that the regular ice crystals observed on 17 February origin from
 354 the surface, because they show a much weaker wind dependency than irregular ice crys-
 355 tals (Fig. reffig:ICNCvsWindHabits1702). This is also observed during one vertical pro-
 356 file (Fig. 10, middle row). The vertical wind speed during this profile was similar for all

heights (3 m s^{-1}), only when the elevator was at a height of 6 m a wind speed reached its maximum of 4.5 m s^{-1} . Whereas the concentration of irregular ice crystals significantly increases at this time and height, the concentration of regular ice crystals gradually decreases with height. This suggests that ice crystals resuspended from the surface have irregular habits and are much more wind dependent.

In this case a different mechanism has to be responsible for the decrease if the ICNC of regular and irregular ice crystals observed on 17 February (Fig. 10). Possibly a turbulent layer above the surface enriches the ICNC of irregular as well as regular ice crystals. In this case surface-based ice-crystal enhancement processes only infrequently increase the ICNC irregular crystals as observed in one profile at a height of 6 m and on 4 February 2017. This also explains why a wind dependency was observed for the irregular ice crystals but not the regular ice crystals. If such an effect is responsible for the decrease of the ICNC, the differences in the size distribution of irregular and regular ice crystals can still not fully be explained. The differences between the irregular ice crystals and the observations of blowing snow by *Nishimura and Nemoto* [2005] is possibly due to the missing sublimation of ice crystals in cloud as it was observed in this study. This can explain the observation of a constant mean diameter with height, whereas the mean diameter in dry air decreased. An explanation of the decrease of the mean diameter of the regular ice crystals can not be given at this point and further observations are necessary to fully understand the findings of this study.

5 Conclusion

This study assess the potential influence of mountain-top in-situ measurements by surface-based ice-crystal enhancement processes and possible implications on the relevance of such measurements for atmospheric studies. For this, an elevator was attached to the meteorological tower of the SBO, Austria and vertical profiles of the ICNC were observed with the holographic imager HOLIMO on two days in February 2017. The main findings are:

- A decrease of the ICNC by at least a factor of two is observed, if the maximum ICNC is larger than 100 l^{-1} . This decrease extended up to one order of magnitude during in cloud conditions and reached its maximum of more than two orders of magnitudes when the station was not in cloud.
- Irregular ice crystals show a stronger wind dependency than regular ice crystals. This is agreement with the observation that surface-based ice-crystals enhancement processes dominantly produce irregular ice crystals.
- On 17 February a similar decrease of the concentration of irregular and regular ice crystals is observed, which can not be explained by surface-based ice crystal enhancement processes. Possibly turbulent layer close to the surface contributes to an enriched ICNC.
- Based on the results of this study, in-situ measurements of the ICNC at mountain-top research stations close to the surface over estimate the ICNC by at least a factor of two. This limits the atmospheric relevance of such measurements. However, the data set obtained is to small to make a clear statement under which conditions in-situ measurements at mountain-top research station may well represent the real properties of a cloud in contact with the surface and when not.
- Further and more extensive field campaigns are necessary to better understand the mechanisms, which are responsible for the enhanced ICNC observed close to the surface at mountain-top research stations. Especially the reason for an increased concentration of irregular ice crystals near the surface is not understood. We propose to perform measurements with a tethered balloon system to extend vertical profiles and better understand possible mechanisms, which enhance the ICNC observed at mountain-top research stations.

408 **Acronyms**

- 409 **ICNC** Ice Crystal Number Concentration
 410 **HOLIMO** HOLographic Imager for Microscopic Objects
 411 **SBO** Sonnblick Observatory

412 **Acknowledgments**

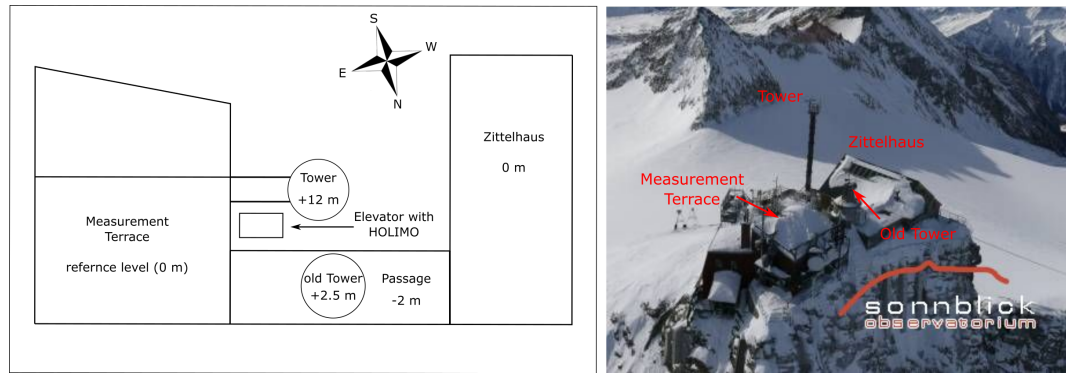
413 Sonnblick Observatory and team (Elke Ludewig, Hermann Scheer, Norbert Daxbacher,
 414 Lug Rasser, Hias Daxbacher)

415 Thanks to Hannes, Olga, Fabiola, Monika, for their help
 416 Thanks to Rob for many discussions

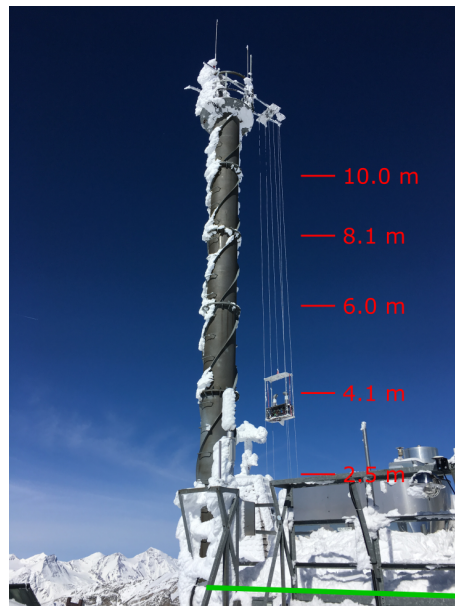
417 **References**

- 418 Baumgardner, D., J. Brenguier, A. Bucholtz, H. Coe, P. DeMott, T. Garrett, J. Gayet,
 419 M. Hermann, A. Heymsfield, A. Korolev, M. KrÃdmer, A. Petzold, W. Strapp,
 420 P. Pilewskie, J. Taylor, C. Twohy, M. Wendisch, W. Bachalo, and P. Chuang (2011),
 421 Airborne instruments to measure atmospheric aerosol particles, clouds and radiation:
 422 A cook's tour of mature and emerging technology, *Atmos. Res.*, 102(1â€§2), 10 – 29,
 423 doi:10.1016/j.atmosres.2011.06.021.
- 424 Beck, A., J. Henneberger, S. Schöpfer, J. Fugal, and U. Lohmann (2017), Hologondel, *At-*
 425 *mos. Meas. Tech.*
- 426 Bromwich, D. H. (1988), Snowfall in high southern latitudes, *Reviews of Geophysics*,
 427 26(1), 149–168, doi:10.1029/RG026i001p00149.
- 428 Budd, W. F. (2013), *The Drifting of Nonuniform Snow Particles1*, pp. 59–70, American
 429 Geophysical Union, doi:10.1029/AR009p0059.
- 430 Déry, S. J., and M. K. Yau (1999), A climatology of adverse winter-type weather
 431 events, *Journal of Geophysical Research: Atmospheres*, 104(D14), 16,657–16,672, doi:
 432 10.1029/1999JD900158.
- 433 Farrington, R. J., P. J. Connolly, G. Lloyd, K. N. Bower, M. J. Flynn, M. W. Gallagher,
 434 P. R. Field, C. Dearden, and T. W. Choularton (2015), Comparing model and measured
 435 ice crystal concentrations in orographic clouds during the inupiaq campaign, *Atmos.*
Chem. and Phys., 15(18), 25,647–25,694, doi:10.5194/acpd-15-25647-2015.
- 436 Field, P. R., R. P. Lawson, P. R. A. Brown, G. Lloyd, C. Westbrook, D. Moisseev, A. Mil-
 437 tenberger, A. Nenes, A. Blyth, T. Choularton, P. Connolly, J. Buehl, J. Crosier, Z. Cui,
 438 C. Dearden, P. DeMott, A. Flossmann, A. Heymsfield, Y. Huang, H. Kalesse, Z. A.
 439 Kanji, A. Korolev, A. Kirchgaessner, S. Lasher-Trapp, T. Leisner, G. McFarquhar,
 440 V. Phillips, J. Stith, and S. Sullivan (2017), Secondary ice production: Current state of
 441 the science and recommendations for the future, *Meteorological Monographs*, 58, 7.1–
 442 7.20, doi:10.1175/AMSMONOGRAPH-D-16-0014.1.
- 443 Fugal, J. P. (2017), Holosuite, in preparation.
- 444 Geerts, B., B. Pokharel, and D. a. R. Kristovich (2015), Blowing Snow as a Natural
 445 Glaciogenic Cloud Seeding Mechanism, *Mon. Weather Rev.*, 143(12), 5017–5033, doi:
 446 10.1175/MWR-D-15-0241.1.
- 447 Gultepe, I., G. Isaac, and S. Cober (2001), Ice crystal number concentration versus tem-
 448 perature for climate studies, *International Journal of Climatology*, 21(10), 1281–1302,
 449 doi:10.1002/joc.642.
- 450 Hallet, J., and S. Mossop (1974), Production of secondary ice particles during the riming
 451 process, *Nature*, 249, 26–28, doi:10.1038/249026a0.
- 452 Lachlan-Cope, T., R. Ladkin, J. Turner, and P. Davison (2001), Observations of cloud and
 453 precipitation particles on the avery plateau, antarctic peninsula, *Antarctic Science*, 13(3),
 454 339â€§348, doi:10.1017/S0954102001000475.

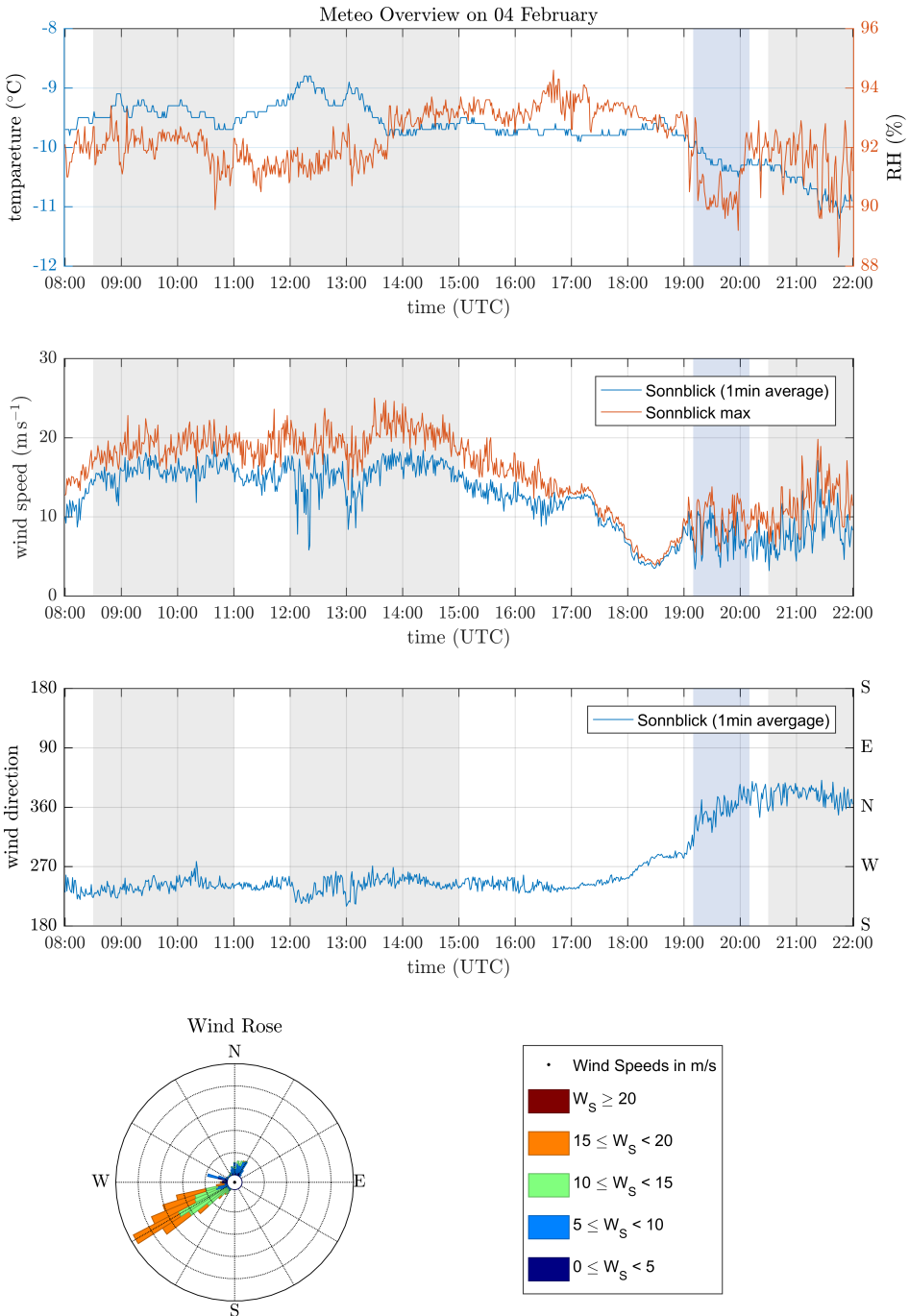
- 456 Li, L., and J. W. Pomeroy (1997), Estimates of threshold wind speeds for snow trans-
 457 port using meteorological data, *Journal of Applied Meteorology*, 36(3), 205–213, doi:
 458 10.1175/1520-0450(1997)036<0205:EOTWSF>2.0.CO;2.
- 459 Lloyd, G., T. W. Choularton, K. N. Bower, M. W. Gallagher, P. J. Connolly, M. Flynn,
 460 R. Farrington, J. Crosier, O. Schlenczek, J. Fugal, and J. Henneberger (2015), The ori-
 461 gins of ice crystals measured in mixed-phase clouds at the high-alpine site jungfraujoch,
 462 *Atmos. Chem. Phys.*, 15(22), 12,953–12,969, doi:10.5194/acp-15-12953-2015.
- 463 Lohmann, U. (2002), Possible aerosol effects on ice clouds via contact nucle-
 464 ation, *Journal of the Atmospheric Sciences*, 59(3), 647–656, doi:10.1175/1520-
 465 0469(2001)059<0647:PAEOIC>2.0.CO;2.
- 466 Mahesh, A., R. Eager, J. R. Campbell, and J. D. Spinhirne (2003), Observations of blow-
 467 ing snow at the south pole, *Journal of Geophysical Research: Atmospheres*, 108(D22),
 468 n/a–n/a, doi:10.1029/2002JD003327, 4707.
- 469 Nishimura, K., and M. Nemoto (2005), Blowing snow at mizuho station, antarctica, *Phi-
 470 losophical Transactions of the Royal Society of London A: Mathematical, Physical and En-
 471 gineering Sciences*, 363(1832), 1647–1662, doi:10.1098/rsta.2005.1599.
- 472 Palm, S. P., Y. Yang, J. D. Spinhirne, and A. Marshak (2011), Satellite remote sensing of
 473 blowing snow properties over antarctica, *Journal of Geophysical Research: Atmospheres*,
 474 116(D16), n/a–n/a, doi:10.1029/2011JD015828, d16123.
- 475 Rangno, A. L., and P. V. Hobbs (2001), Ice particles in stratiform clouds in the arctic and
 476 possible mechanisms for the production of high ice concentrations, *Journal of Geophysi-
 477 cal Research: Atmospheres*, 106(D14), 15,065–15,075, doi:10.1029/2000JD900286.
- 478 Rogers, D. C., and G. Vali (1987), Ice crystal production by mountain sur-
 479 faces, *J. Clim. Appl. Meteorol.*, 26(9), 1152–1168, doi:10.1175/1520-
 480 0450(1987)026<1152:ICPBMS>2.0.CO;2.
- 481 Rotunno, R., and R. A. Houze (2007), Lessons on orographic precipitation from the
 482 mesoscale alpine programme, *Quarterly Journal of the Royal Meteorological Society*,
 483 133(625), 811–830, doi:10.1002/qj.67.
- 484 Schlenzeck, O., and J. Fugal (2017), Microphysical properties of ice crystal precipitation
 485 and surface-generated ice crystals in a high alpine environment in switzerland, *esult*, 56,
 486 433–453, doi:10.1175/JAMC-D-16-0060.1.
- 487 Schmidt, R. A. (1982), Vertical profiles of wind speed, snow concentration, and
 488 humidity in blowing snow, *Boundary-Layer Meteorology*, 23(2), 223–246, doi:
 489 10.1007/BF00123299.
- 490 Vali, G., D. Leon, and J. R. Snider (2012), Ground-layer snow clouds, *Quarterly Journal
 491 of the Royal Meteorological Society*, 138(667), 1507–1525, doi:10.1002/qj.1882.
- 492 Vionnet, V., G. GuyomarcâŽh, F. N. Bouvet, E. Martin, Y. Durand, H. Bellot, C. Bel,
 493 and P. PugliÃlse (2013), Occurrence of blowing snow events at an alpine site over a
 494 10-year period: Observations and modelling, *Advances in Water Resources*, 55, 53 – 63,
 495 doi:<http://doi.org/10.1016/j.advwatres.2012.05.004>, snowâŠAtmosphere Interactions
 496 and Hydrological Consequences.
- 497 Yang, J., and M. K. Yau (2008), A new triple-moment blowing snow model, *Boundary-
 498 Layer Meteorology*, 126(1), 137–155, doi:10.1007/s10546-007-9215-49.



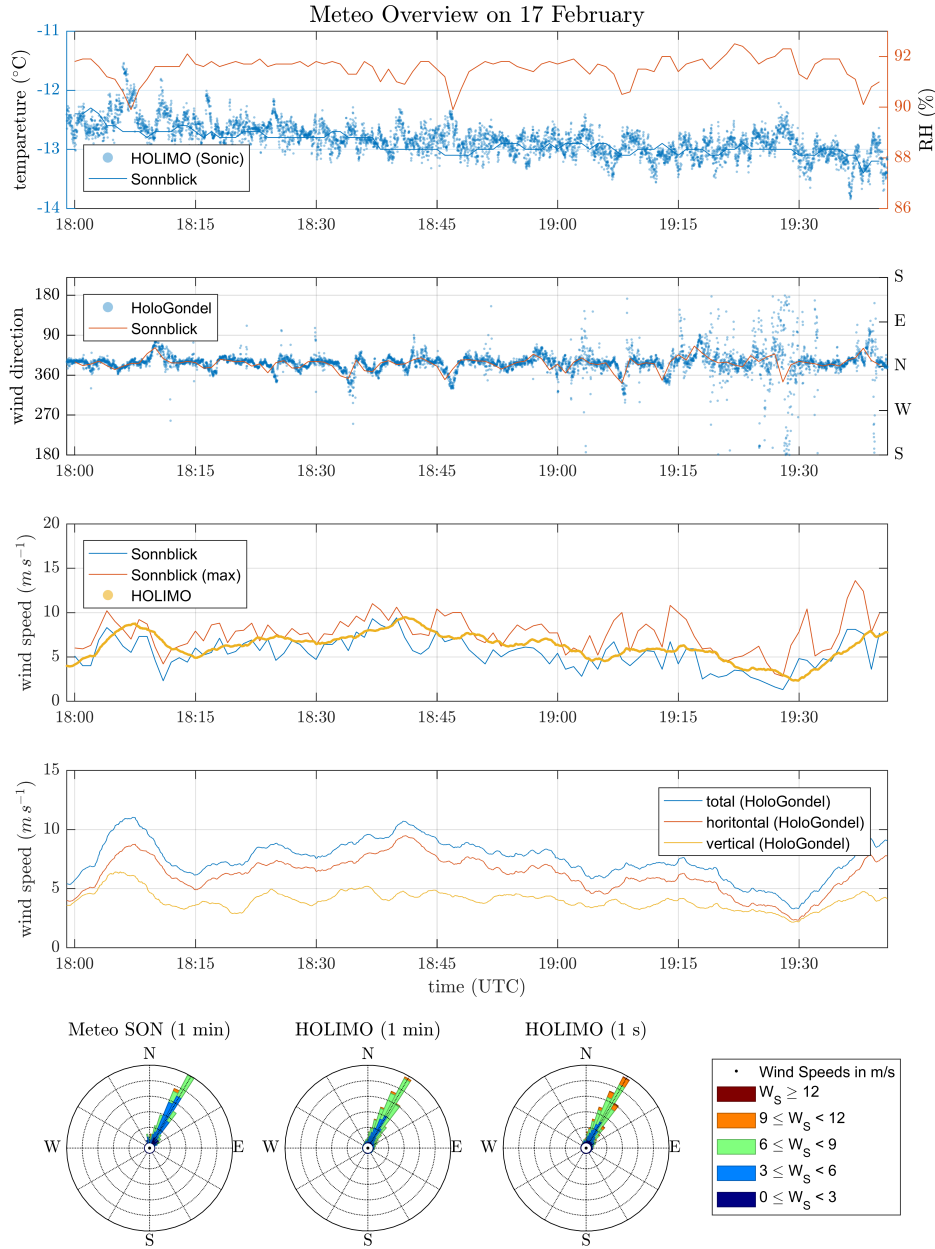
499 **Figure 1.** Sketch of the experimental setup and the surrounding structures (left) with their heights relative
500 to the bottom of the measurement terrace. Aerial image of the Sonnblick Observatory (right).



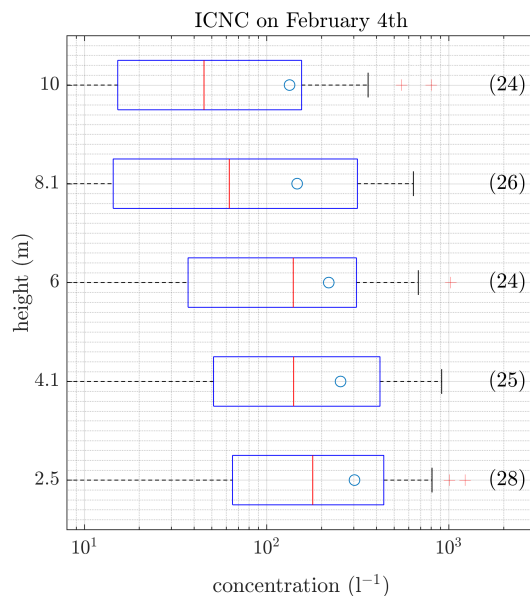
501 **Figure 2.** Set up of the elevator with the holographic imager HOLIMO mounted to the meteorological
502 tower at the SBO. The red lines and numbers indicate the five different heights where the elevator was posi-
503 tioned repeatedly to obtain vertical profiles of the ICNC. The reference height of 0.0 m is the bottom of the
504 measurement platform (green line).



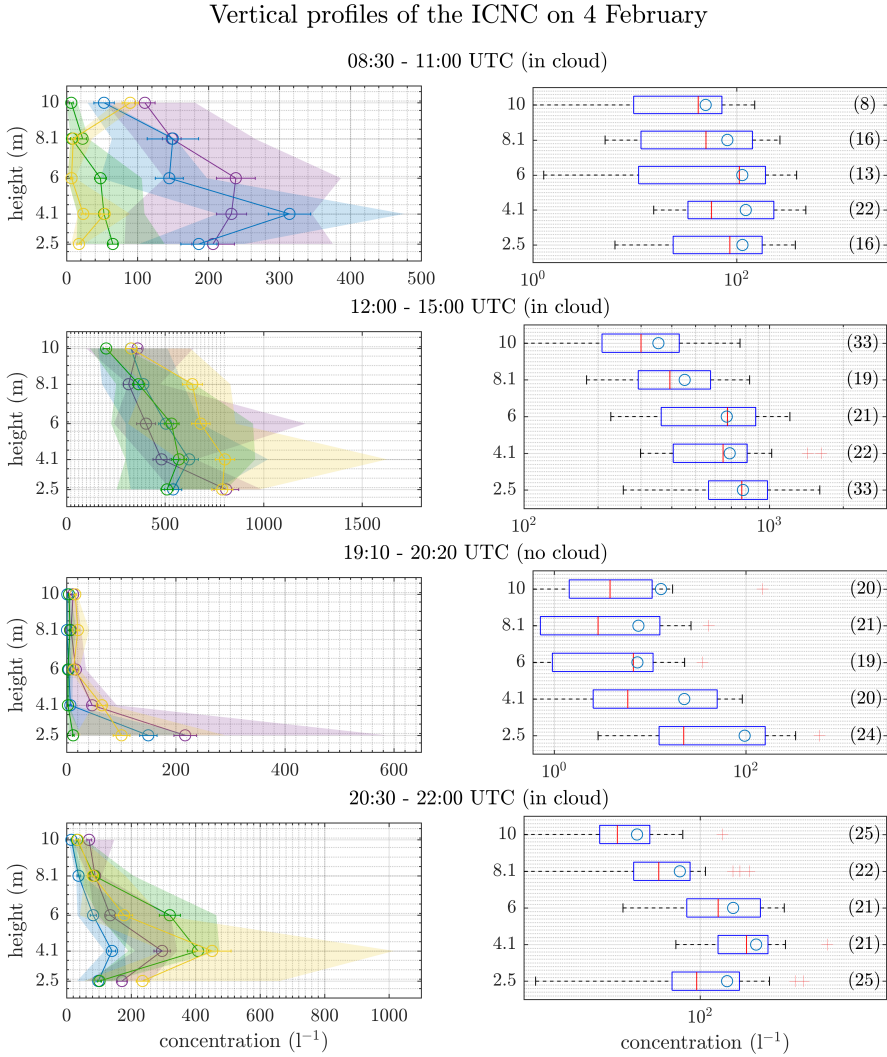
505 **Figure 3.** Overview of the meteorological conditions on 4 February obtained from the SBO measurements.
506 Shown are the temperature, relative humidity (top), wind speed (second from top) and wind direction (second
507 from bottom). All measurements are 1 min averages except for the maximum wind speed, which corresponds
508 to the maximum wind speed observed during a corresponding 1 min average. Grey and blue shaded areas
509 represent time with measurement (see Fig. 6) when the SBO was in cloud, respectively not in cloud. A wind
510 rose plot (bottom) of the wind measurement is also shown.



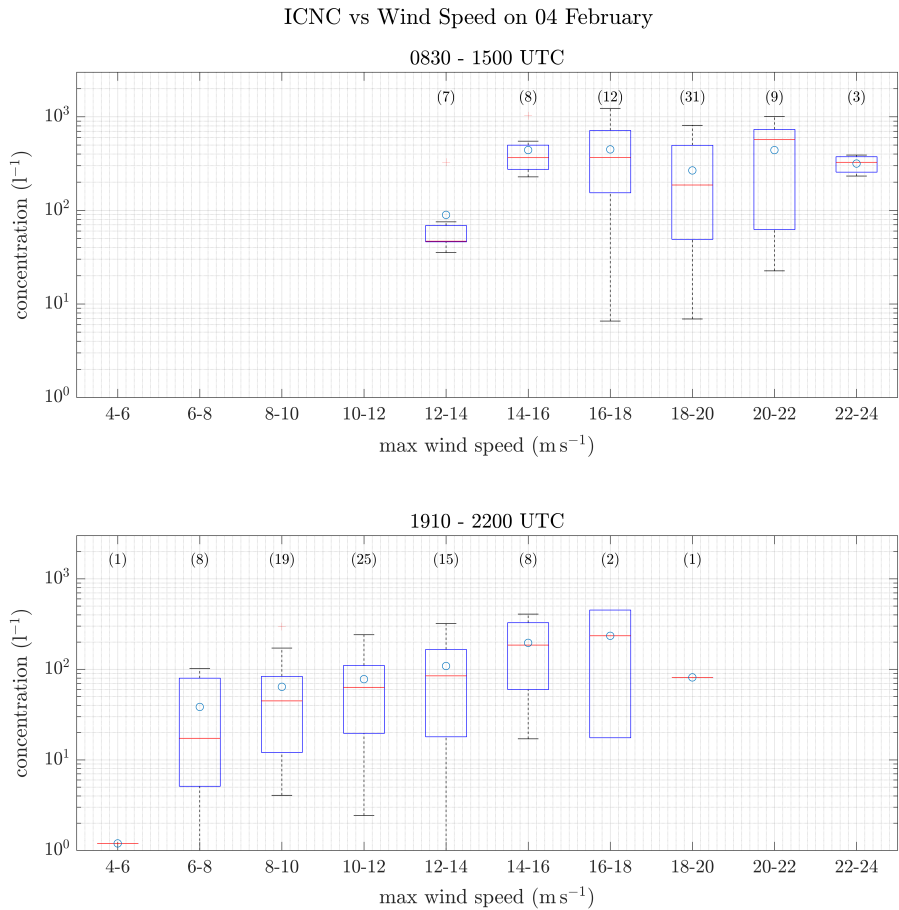
511 **Figure 4.** Overview on the meteorological conditions on 17 February for the time interval when measure-
 512 ments exist (see Fig. 8). On this day temperature and wind measurements are available from the SBO and the
 513 3D Sonic Anemometer. Shown are the temperature and relative humidity (top), wind direction (second from
 514 top), a comparison of the horizontal wind speed (middle) and detailed wind speed measurements from the 3D
 515 Sonic Anemometer (second from bottom). A windrose plot is shown in the bottom panel.



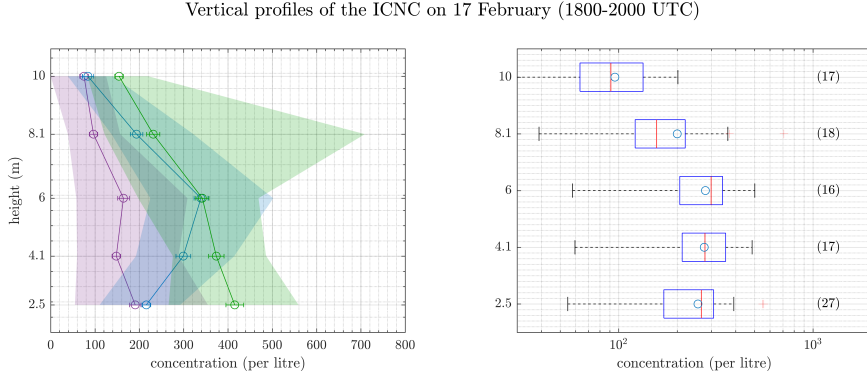
516 **Figure 5.** ICNC as a function of the height of the elevator at the meteorological tower of the SBO. This plot
 517 is a summary of the 24 profiles obtained on 4 February. The data was averaged over the entire time period
 518 of single measurements at the different height. The number in brackets is the number of concentration
 519 measurements per height. For each box, the central line marks the median value of the measurement and the
 520 left and right edges of the box represent 25th and the 75th percentiles respectively. The whiskers extend to
 521 minimum and maximum of the data; outliers are marked as red pluses. The mean value of the measurements
 522 is indicated as a blue circle.



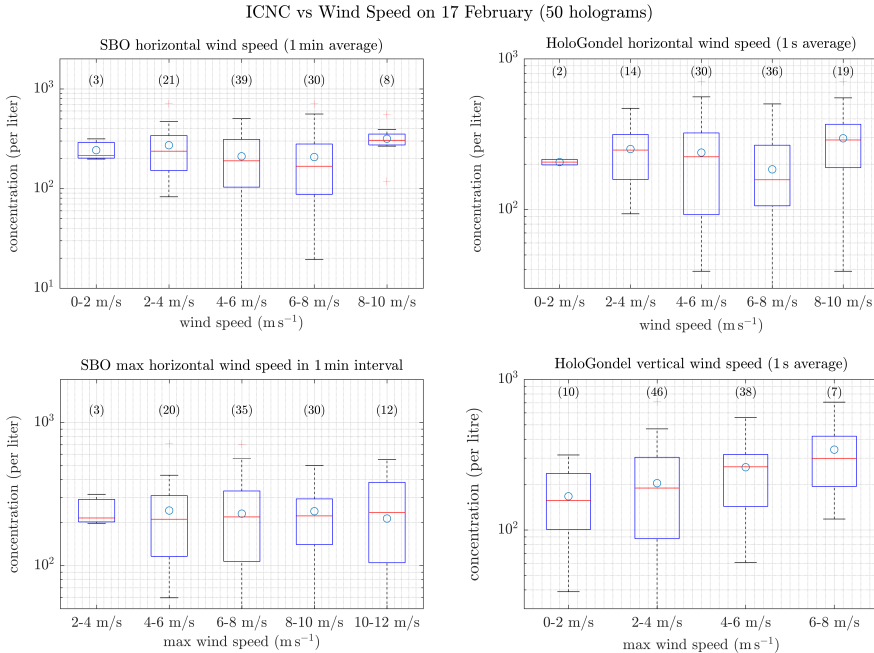
523 **Figure 6.** ICNCs as a function of height of the elevator for four different time intervals during 4 February,
 524 representing different conditions (Fig. 3). On the individual profiles (left), the circles indicate the mean value
 525 averaged over the entire time interval. The error bars represent the standard error of the mean. The shaded
 526 area extends from the minimum to the maximum of the measured ICNC. As in Fig. 5 only for the four time
 527 intervals the box plots (right) show a summary of the data.



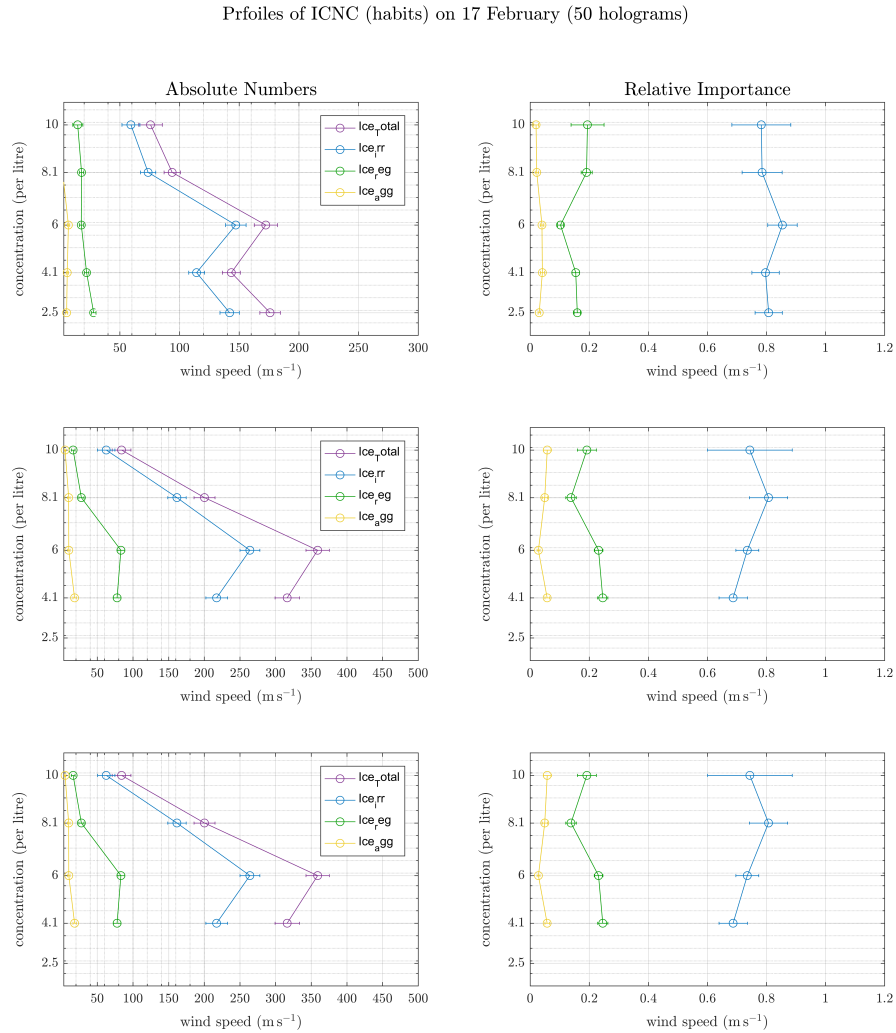
528 **Figure 7.** As Figure 5 only ICNC as a function of horizontal wind speed for the the time periods between
 529 0830 and 1500 UTC when the wind direction was West-Southwest (top) and between 1910 and 2200 UTC
 530 when the wind direction was North (bottom). The wind speed is the maximum wind speed in one minute time
 531 intervals from the SBO.



532 **Figure 8.** Ice crystal number concentration as a function of the height of the elevator at the meteorological
 533 tower of the SBO for 17 February. On the left are the three individual profiles obtained in cloud. The circles
 534 indicate the mean value averaged over the entire time interval. The error bars represent the standard error of
 535 the mean. The shaded area indicates the variability of the data and extends from the minimum to the maxi-
 536 mum when the data is averaged over 50 holograms. For the summary of the different time intervals (right) the
 537 data is averaged over 50 holograms. For each box, the central line marks the median value of the measurement
 538 and the left and right edges of the box represent 25th and the 75th percentiles respectively. The whiskers
 539 extend to minimum and maximum of the data; outliers are marked as red pluses.



540 **Figure 9.** As Figure 7 only for 17 February and four different wind speed measurements: a) one minute
 541 averages of the horizontal wind speed from the SBO, b) maximum wind speed of the a corresponding time
 542 interval in a), c) secondly averages of the horizontal wind speed and d) secondly average of the vertical wind
 543 speed both from the 3D Sonic Anemometer.



544 **Figure 10.** Vertical profiles of the concentration (left) and the relative importance (right) of the subclassified ice crystal habits: regular, irregular and aggregates. For the relative importance the number of ice crystals
 545 of different habits were divided by the total number of ice crystals. For theses plots the data as averaged
 546 over 50 holograms. In both cases the circles represent the mean of the 50 hologram averages. The error bars
 547 represent the standard error of the mean.
 548

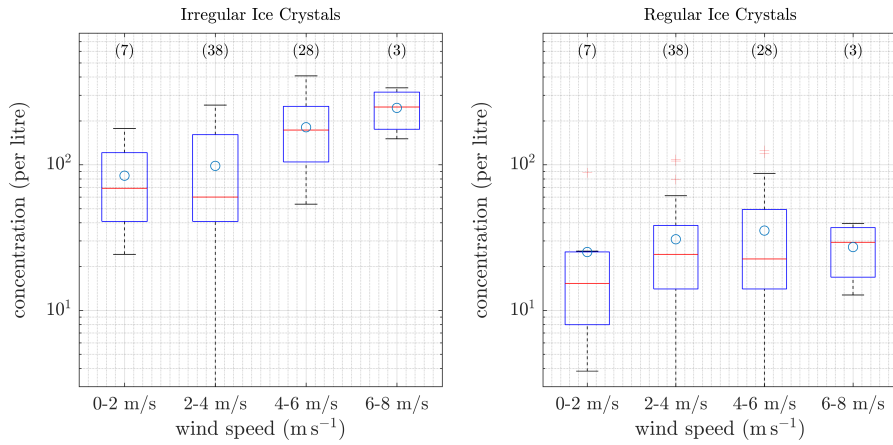


Figure 11. As Figure 7 only for 17 February and the ICNC of different ice crystal habits as a function of the vertical wind speed.

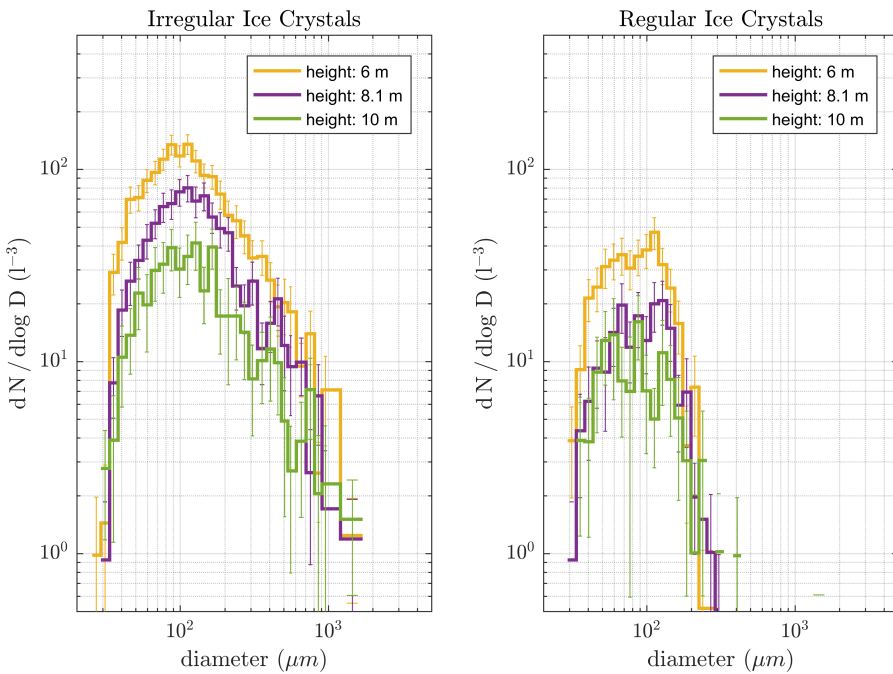
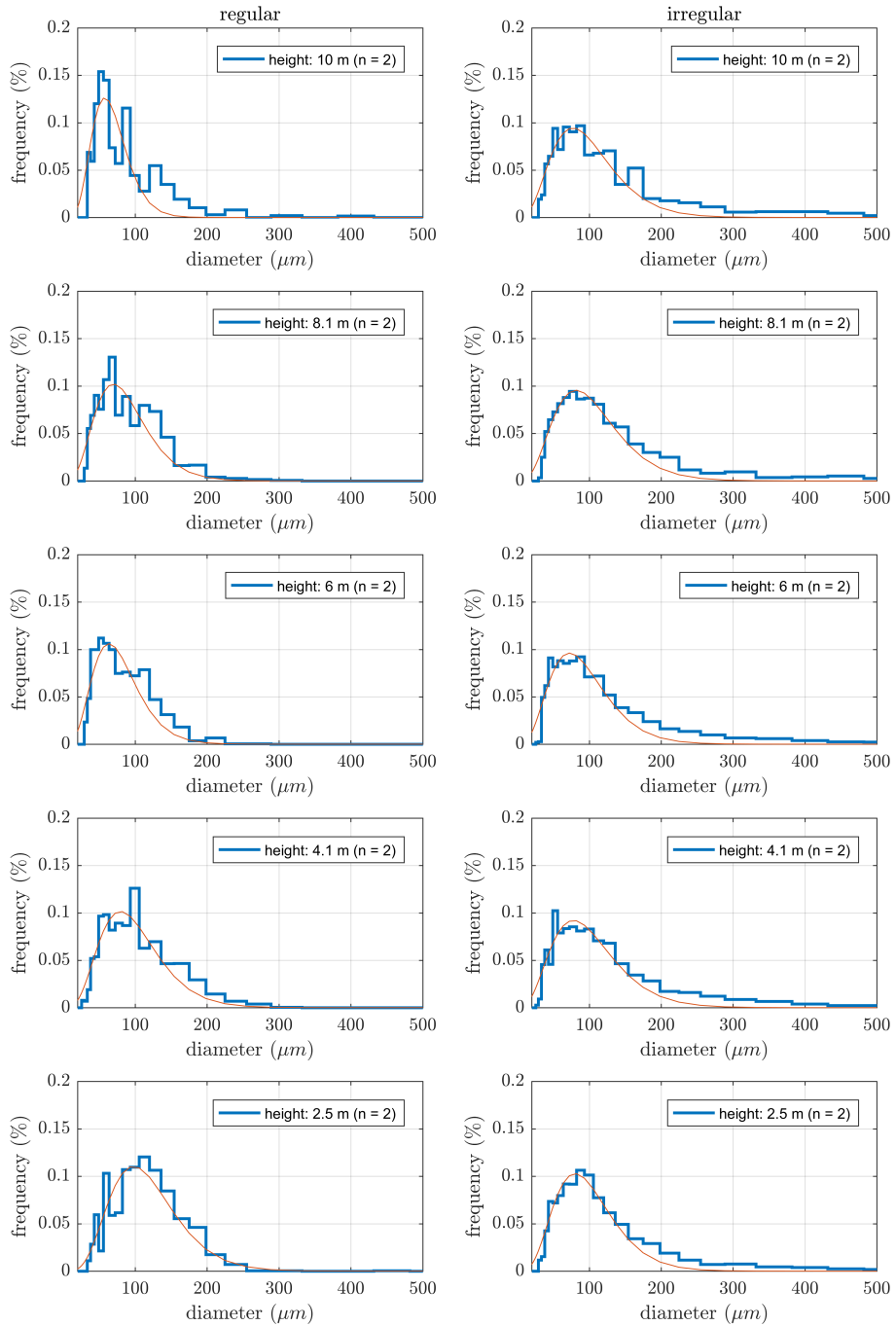
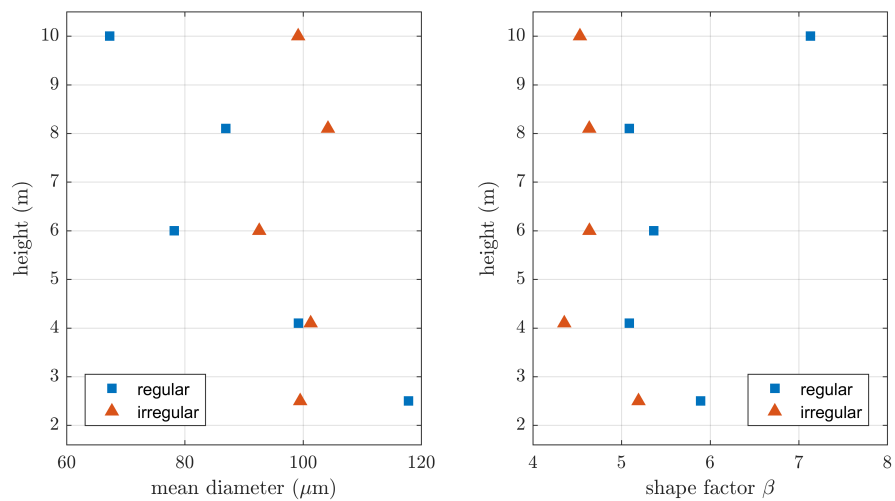


Figure 12. Size distribution of the irregular (left) and regular (right) ice crystals observed on 17 February as a function of height. The errorbars represent the standard error of the mean.



553 **Figure 13.** Probability distribution of the particle diameter for regular (left)
554 and irregular (right) ice crystals
555 measured on 17 February. The red line indicates the result of the fit of the two parameter gamma-pdf from
equation (1).



556 **Figure 14.** Profiles of the mean diameter (left) and the shape parameter (right)
557 of the two parameter gamma-pdf (Eq. (1)) plotted as a function of height.